Title: A Gaussian process and image registration based stitching method for high dynamic range measurement of precision surfaces

Authors: M.Y. Liu, C.F. Cheung, C.H. Cheng, R. Su, R.K. Leach

PII: S0141-6359(16)30137-4
DOI: http://dx.doi.org/doi:10.1016/j.precisioneng.2017.04.017
Reference: PRE 6569

To appear in: *Precision Engineering*

Received date: 4-8-2016
Revised date: 24-2-2017
Accepted date: 24-4-2017

Please cite this article as: Liu MY, Cheung CF, Cheng CH, Su R, Leach R.K.A Gaussian process and image registration based stitching method for high dynamic range measurement of precision surfaces.*Precision Engineering* http://dx.doi.org/10.1016/j.precisioneng.2017.04.017

A Gaussian process and image registration based stitching method for high dynamic range measurement of precision surfaces

M. Y. Liu[a,b], C. F. Cheung[a,*], C. H. Cheng[a], R. Su[b], and R. K. Leach[b]

[a]Partner State Key Laboratory of Ultra-precision Machining Technology, Department of Industrial and Systems Engineering, The Hong Kong Polytechnic University, Kowloon, Hong Kong, China
[b]Manufacturing Metrology Team, Faculty of Engineering, University of Nottingham, University Park, Nottingham NG7 2RD, United Kingdom
[*]benny.cheung@poylu.edu.hk

Highlights:

- It makes use of Gaussian process to model the sub-aperture measurement datasets to obtain the mean surface for registration, which is a novel method as comparing to traditional filtering methods, and provides better registration accuracy.
- Image registration and z shift method are used to simplify the 6 degrees of freedom 3D point cloud registration to a 3 degrees of freedom registration.
- Edge intensity data fusion method is used to fuse the overlapped region to provide a better transition between two datasets.
- It provides a novel stitching solution for a wide range of optical measurement instruments for achieving high dynamic range optical measurement of precision surfaces

Abstract: Optical instruments are widely used for precision surface measurement. However, the dynamic range of optical instruments, in terms of measurement area and resolution, is limited by the characteristics of the imaging and the detection systems. If a large area with a high resolution is required, multiple measurements need to be conducted and the resulting datasets needs to be stitched together. Traditional stitching methods use six degrees of freedom for the registration of the overlapped regions, which can result in high computational complexity. Moreover, measurement error increases with increasing measurement data. In this paper, a stitching method, based on a Gaussian process, image registration and edge intensity

data fusion, is presented. Firstly, the stitched datasets are modelled by using a Gaussian process so as to determine the mean of each stitched tile. Secondly, the datasets are projected to a base plane. In this way, the three-dimensional datasets are transformed to two-dimensional (2D) images. The images are registered by using an (x, y) translation to simplify the complexity. By using a high precision linear stage that is integral to the measurement instrument, the rotational error becomes insignificant and the cumulative rotational error can be eliminated. The translational error can be compensated by the image registration process. The z direction registration is performed by a least-squares error algorithm and the (x, y, z) translational information is determined. Finally, the overlapped regions of the measurement datasets are fused together by the edge intensity data fusion method. As a result, a large measurement area with a high resolution is obtained. A simulated and an actual measurement with a coherence scanning interferometer have been conducted to verify the proposed method. The stitching result shows that the proposed method is technically feasible for large area surface measurement.

Keywords: Surface measurement; stitching; high dynamic range; Gaussian process; image registration

1. Introduction

In precision metrology, one challenge is the high dynamic range measurement of precision surfaces, which require both large measurement area and high resolution data [1]. This is especially true for the measurement of surfaces with multi-scale characteristic which have large scale topographic and small scale structure. Due to the limited field of view (FOV) and resolution of the camera, it is difficult to obtain a result with a satisfactory range in a single measurement which measures multi-scale information. One of the possible solutions is to perform multiple measurements and stitch the results together to form a dataset with a larger area to reveal the large topographic information without losing the high resolution information to characterize the micro-structure pattern [2].

Stitching has been reported for a sub-aperture stitching interferometer for both spherical and flat surface measurements [3-6]. Preibisch et al. [7] used a phase-correlation method to find the translation matrix between image pairs and performed global optimal stitching. Chen et al. [8] proposed a sub-aperture stitching and localization algorithm for spherical and planar surfaces. Moreover, they developed a coarse-to-fine stitching strategy. Zhang et al. [9] developed a simultaneous reverse optimizing reconstruction method which is based on system modelling technique for aspheric sub-aperture stitching interferometer. Ye et al. [10] used an optimal stitching planning method to measure large aspheric optical surface with ±4 mm range of probe and 20% of overlapped region. Wiegmann et al. [11] evaluated the accuracy of the sub-aperture stitching method using virtual experiments and found that the overall accuracy of stitching result outperformed the direct measurement method by a factor of about 3. For surface measurement instruments such as coherence scanning interferometers, which are widely used today for precision surface measurement, some commercial products can provide a stitching function for relatively flat surfaces [12].

However, most of the stitching methods make use of six degrees of freedom for registration in the overlapped regions and the computational complexity is relatively large. For instance, the Iterative Closest Point (ICP) algorithm [13] has $O(N_p N_x)$ complexity for a single iteration. For a registration with N_t and N_q initial translations and rotations, the total complexity is $O(N_p N_x N_t N_q)$ which is considerably high. Moreover, the error caused by the stitching algorithm is accumulated when the number of sub-surface measurements is increasing, especially for the rotational error, which is difficult to compensate. Marinello et. al [14] pointed out that the translational error is biggest source of errors, while the Roll, Pitch and Yaw error can be as small as several arc-sec. With the help of high precision linear stages in which the rotational error can be considered to be minimal or negligible, registration can be simplified to a three degrees of freedom translation problem with the complexity reduced to $O(N_p N_x N_t)$.

In this paper, a stitching method based on Gaussian process and image registration together with an edge intensity data fusion is developed. The working principle of the method is discussed. A simulation and an actual measurement were conducted to verify the method. Some technical aspects are also discussed and the edge effect is improved as compared with the traditional method. The results of the experiments show that the proposed method is suitable for stitching of measurement results of areal measurement instruments, which provides a technically feasible solution for high dynamic range optical measurement for precision surfaces.

2. The principle of the Gaussian process and image registration based stitching method

The framework of the proposed Gaussian process and image registration based stitching method is shown in Fig. 1. First, the sub-aperture measurement datasets are modelled using a Gaussian process [15] so as to obtain the mean surfaces, which can reduce the registration error caused by measurement noise and outliers. The datasets are converted to two-dimensional images and the images are registered using an intensity based algorithm, which can determine the (x, y) translation parameters. The MATLAB Image Registration Toolbox [16] has been used to implement this algorithm. In this study, 20 % overlapped area for the measurement datasets is chosen for the best balance between efficiency and accuracy [17]. After the (x, y) translation is determined, the z axis translation is calculated by using a least-squares error method so as to minimize the z distance between the two mean surfaces. The next step is to calculate the data in the overlapped region with an edge intensity data fusion method. Finally, the datasets are stitched together to form a dataset combining all the (x, y, z) translation information and fused overlapped data.

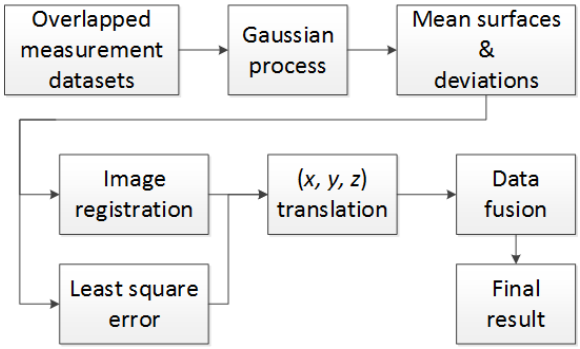

Fig. 1: Diagram of the Gaussian process based stitching method

2.1 Gaussian process modelling of original surfaces

Noise in the measurement processes and outliers in the result may affect the registration accuracy. Huang et al. [18] pointed out that both the standard deviation of the noise and the mean error of the noise have influence of the registration error. Traditional methods utilise filtering techniques to remove noise and outliers in the original measurement results. However, filtering is limited by distortion and edge effects [19]. The Gaussian process modelling involved in the proposed stitching method aims to improve the registration accuracy [20]. The original measurement results can be described as a discrete function of $z(x_i, y_i)$, which means the z-coordinate of the i-th point is a function of the lateral position (x_i, y_i). Let $\mathbf{v}_i = (x_i, y_i)$, so the measured datasets can be represented as $z(\mathbf{v}_i)$, $i = 1, 2, \ldots, N$, where N is the number of points. The measurement process can be considered as a Gaussian process which is a stochastic process, with underlying surface and measurement noise, which can be expressed as

$$z(\mathbf{v}_i) = f(\mathbf{v}_i) + \varepsilon \tag{1}$$

where $f(\mathbf{v}_i)$ is the underlying surface and ε is the measurement noise, which is assumed to have a Gaussian distribution $\varepsilon \sim N(0, \sigma_\varepsilon^2)$, with zero mean and σ_ε^2 variance.

In order to model the underlying surface, Gaussian process modelling is used in this study. A Gaussian process is a random process where the probability distribution function to the associated observation is normal and the joint probability distributions associated with any finite

subset of the observations are also normal. A Gaussian process can be modelled as a mean function and a covariance function, which can be expressed as:

$$f(\mathbf{v}_i) = GP(m_z(\mathbf{v}_i), k_z(\mathbf{v}_i, \mathbf{v}_j)) \tag{2}$$

where $m_z(\mathbf{v}_i)$ is the mean function, $k_z(\mathbf{v}_i, \mathbf{v}_j)$ is the covariance function with $m_z(\mathbf{v}_i) = E[z(\mathbf{v}_i)]$ and $k_z(\mathbf{v}_i, \mathbf{v}_j) = E[(z(\mathbf{v}_i) - m_z(\mathbf{v}_i))(z(\mathbf{v}_j) - m_z(\mathbf{v}_j))]$. The mean function represents the expected *z* value at $\mathbf{v}_i$ while the covariance function represents the variance of the *z* value when $\mathbf{v}_i = \mathbf{v}_j$ and the covariance between the *z* values when $\mathbf{v}_i \neq \mathbf{v}_j$.

In this study, the mean function is designed to be zero function since the measured surface is unknown. Moreover, a squared exponential function is used to represent the covariance of the Gaussian process model:

$$k_z(\mathbf{v}_i, \mathbf{v}_j) = \sigma_z^2 \exp\left(-\frac{\left\| \mathbf{v}_i - \mathbf{v}_j \right\|^2}{2l^2} \right) \tag{3}$$

where $\left\| \mathbf{v}_i - \mathbf{v}_j \right\|$ is the distance between $\mathbf{v}_i$ and $\mathbf{v}_j$, σ_z^2 is the constant variance of the Gaussian process model and *l* is the characteristic length-scale.

The parameters of the covariance function corresponding to unit characteristic length-scale and unit signal standard deviation are first initiated to be zeros and the likelihood parameter was initiated to be $\log(0.1)$, which denotes the standard deviation of the noise to be 0.1 mm. The parameters of the Gaussian process was then optimized by minimizing the negative log marginal likelihood. After the parameters are optimized, the mean surface and the covariance surface of the measured data are fully determined. In this study, the implementation of the Gaussian process modelling is based on the Gaussian processes for machine learning (GPML) toolbox [21].

2.2 Image registration for x-y alignment

After Gaussian process modelling, the mean surfaces of the original measurement datasets are modelled. The three-dimensional datasets are then projected on to the *x-y* plane as 2D images. Image registration is used to align the overlapped images. Generally, there are four types of transformation for image registration, i.e. translation, rigid, similarity and affine. In this study, the translational type is used since only *x-y* translation is considered. The technique used in the image registration process is intensity-based automatic image registration. The intensity-based automatic image registration is an iterative process. Firstly, the overlapped regions of two images are identified, one is set as the fixed image while the other is set as the moving image. Hence, a metric, an optimizer and the transformation type are specified. Since the measurement datasets are taken from the same instrument, the metric and optimizer are configured as monomodal. For each iteration, a transformation matrix applied to the moving image is determined and the metric comparing with the transformed moving image with a bilinear interpolation to the fixed image is determined. The iteration stops when the stop condition is detected, e.g. when it reaches a point of diminishing returns or reaches the maximum number of iterations.

2.3 z axis alignment

In the previous step, the overlapped region is registered in the *x-y* direction. The datasets in *z* axis are then aligned to minimize the distances of the overlapped surfaces. This is a least-squares problem and the objective function can be determined by

$$F = \sum_{i=1}^{N} \left\| z_i' - z_i \right\|^2 \tag{5}$$

where z_i' and z_i are the corresponding points in the two surfaces, and z_i' denotes the translated data points of the alignment process along the *z* axis. Translation in the *z* axis can be calculated by minimizing the objective function in Eq. (5).

2.4 Data fusion for the overlapped area

When all the (*x*, *y*, *z*) translation information is determined, the datasets can be stitched together to form an overall measurement result. For the overlapped region, the data is fused together with a data fusion algorithm. There are many kinds of data fusion methods such as simple or weighted means, weighted least-squares fusion and residual approximation-based fusion [22]. In this study, the edge intensity data fusion method [23] is used. For a dataset $R(m\times n)$, the edge intensity is defined by

$$E_{R(i,j)} = \left| \frac{f(i,j) - \bar{m}}{m \times n - 1} \right| \tag{6}$$

where $\bar{m} = \sum_{i=1}^{n} \sum_{j=1}^{m} \frac{f(i,j)}{m \times n}$ ($i = 1,...,n$, $j = 1,...,m$)

For two datasets $A(i,j)$ and $B(i,j)$, the weighting functions are determined by

$$\begin{cases} W_{A(i,j)} = \dfrac{E_{AR(i,j)}}{E_{AR(i,j)} + E_{BR(i,j)}} \\ W_{B(i,j)} = \dfrac{E_{BR(i,j)}}{E_{AR(i,j)} + E_{BR(i,j)}} \end{cases} \tag{7}$$

Hence, the fused dataset *F* is determined by

$$F(i,j) = W_{A(i,j)} \times A(i,j) + W_{B(i,j)} \times B(i,j) \tag{8}$$

3. Simulation verification

To verify the proposed stitching method, a simulation using MATLAB was conducted. As shown in Fig. 2, a synthetic large sinusoidal surface was considered as the targeted measuring surface. The design of the surface is determined by

$$\mathrm{z} = \frac{\sin(x) + \cos(y)}{500} + GN(0, 0.1) \tag{9}$$

where $GN(0, 0.1)$ is the added Gaussian noise with zero mean and 0.1 μm variance.

The peak-to-valley distance of the surface was 8 µm. The area of the whole surface was (100×100) mm which was divided into nine sub-regional measurements. The highlighted area in Fig. 2 denotes the overlapped area between nearby measurement datasets.

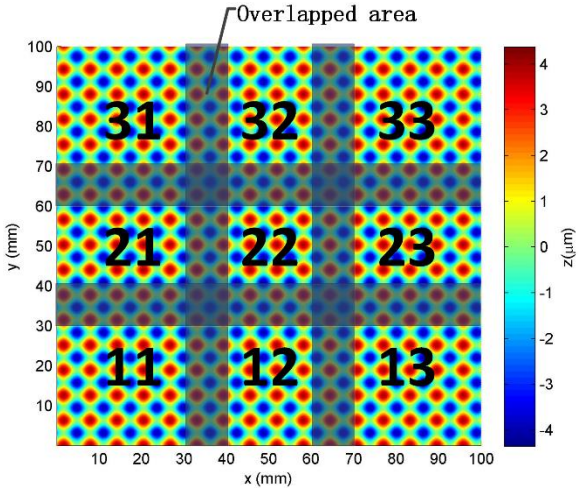

Fig. 2: Simulated stitching surface

As shown in Fig. 2, the nine measurements have the same size and are marked as 11~13, 21~23 and 31~33 respectively. The area of the individual measurement was (40×40) mm while the width of the overlapped area (highlighted in the figure) was 8 mm, which was 20 % of the width of the dataset, as suggested elsewhere [17].

After the Gaussian process, the mean and variance of the original surface were determined and Fig. 3 shows the mean and variance of surface 11. The result shows that the standard deviation of the majority of the modelled surface is about 0.1 µm, while the simulated noise level is 0.1 µm, which demonstrates the effectiveness of the Gaussian process.

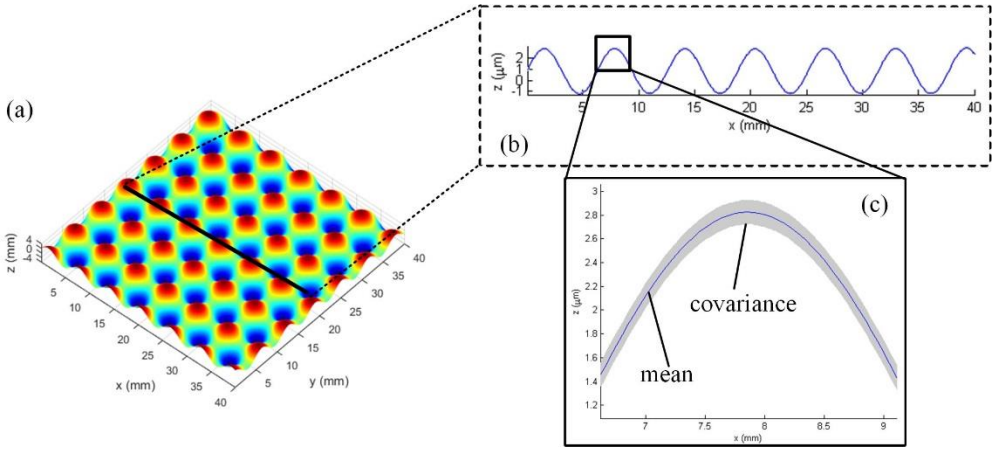

Fig. 3: Results after Gaussian process. (a) original surface, (b) 2D section profile illustrating mean and covariance, (c) zoom-in view of mean and covariance

The mean surfaces after Gaussian process modelling were then transformed into 2D grayscale images to perform image registration. The registration result of the overlapped regions of surface 11 and surface 12 are shown in Fig. 4. The result shows that the two sub-regions are well registered.

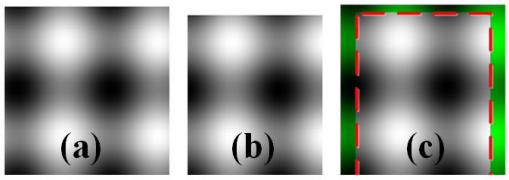

Fig. 4 Zoom-in view of one pair the registration results. (a) fixed image, (b) moving image, (c) registered pair images

After image registration, the (*x*,*y*) translation relationship of the nearby regions was determined. The next step was to register the datasets in the *z* direction. The process was to search for the minimum distance between the two mean surfaces by using the least-squares error method. For surface region 11 and surface region 12, the aligned result is shown in Fig. 5. The result shows that the two surfaces are well registered in the *z* direction.

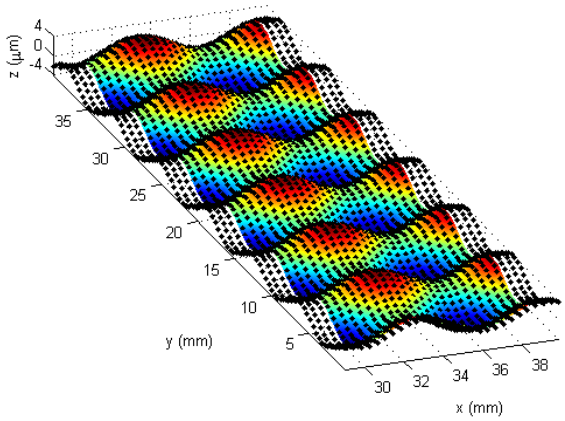

Fig. 5: *z* axis registration result. The colour-coded surface represents surface 11 and the black dots represents surface 12

After the (*x*, *y*, *z*) translation information was determined, the sub-regions could be stitched together. The data in the overlapped area was recalculated with the edge intensity method. Fig. 6 shows the final stitching result. Fig. 6 shows that there are no obvious edges in the overlapped area, which indicates that the datasets are well stitched. The final stitching result is also registered to the original design surface with an iterative closest point (ICP) method [13] and the error map is determined as shown in Fig. 7. The root-mean-square (RMS) value of the error map is 0.108 μm. The error map shows that the error is evenly distributed and in most areas is close to zero. It is also interesting to note that the error in the centre area is relatively small compared to that in the surrounding areas. This is mainly caused by the accumulated errors in the image registration process since the surrounding datasets principally need more connections than those in the centre. The different patterns for the error map related to two nearby sub-surfaces are the results from the registration error for the proposed method. The result shows that the registration error is in the level of sub-micrometer and the error for each nearby registration is randomly distributed, which depends on the data in the overlapped area. This is well demonstrated in different datasets for x direction, i.e. for different groups of datasets (11,

12, 13), (21, 22, 23) and (31, 32, 33), the errors are distributed (from left to right) in a increasing manner, first decreasing and then increasing manner, and decreasing manner, respectively.

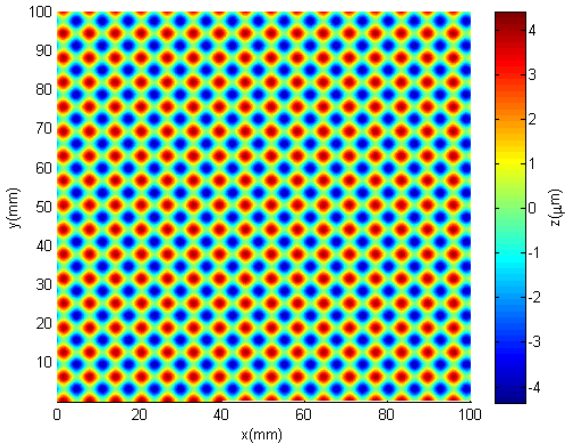

Fig. 6: Stitching result

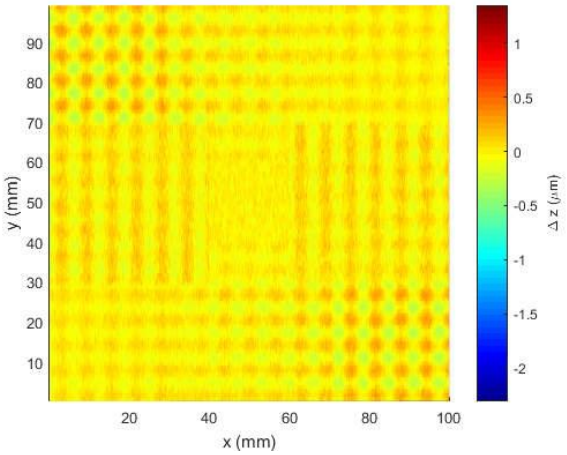

Fig. 7: Error map comparing with the design surface

4. Experimental verification and discussion

4.1 Measurement of a diamond-turned sinusoidal surface

To demonstrate the practical usage of the proposed method, a stitching measurement experiment was conducted by measuring a diamond-turned sinusoidal surface by a commercial coherence scanning interferometer (CSI, with a

20× object lens and 1× and 0.55× zoom lens). The surface was measured in a manner similar to the simulation in a 3×3 matrix arrangement. The area of a single measurement is approximately (0.3×0.2) mm. A set of nearby sub-surfaces with an overlap marked region is shown in Fig. 8 and all the original measurement data is shown in Fig. 9.

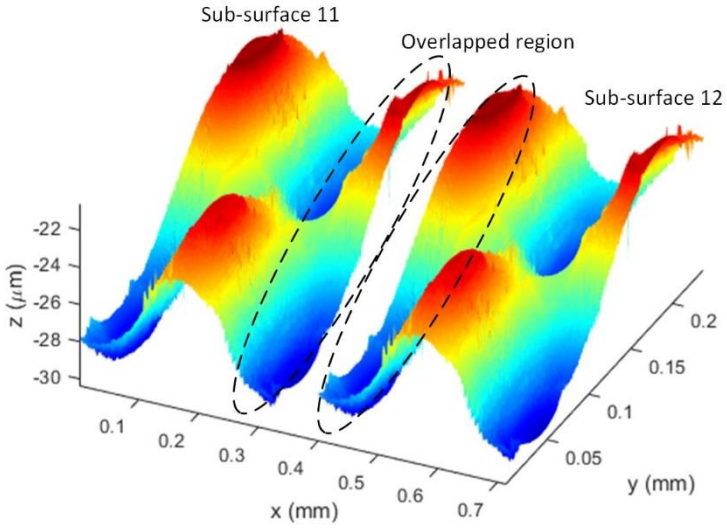

Fig. 8: The 3D dataset for two nearby sub-surfaces, the overlap region is marked with dash line

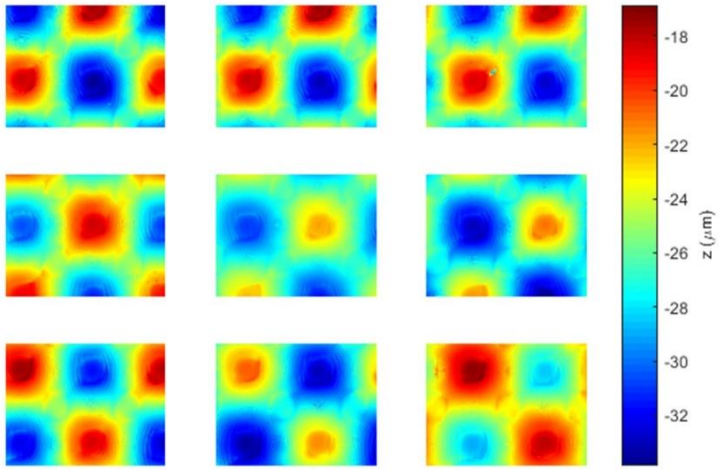

Fig. 9: Original data (measurement size of each dataset is approximately (0.3×0.2) mm and the colour bar gives height information in micrometres)

After obtaining the individual measurement data, the data was modelled by a Gaussian process. The mean surfaces of the measurement data are shown in Fig. 10. The result shows that the overall deviations of the mean surfaces are greatly reduced and the intensities of the subfigures have better uniformity. This result demonstrates the advantage of using a Gaussian process to model the measurement data, especially when the measurement noise is large or the measurement result is affected by obstacles such as dusts and/or scratches. As reported by Huang et al. [18], the registration error is about 25 µm for a noise level with standard deviation of 150 µm,.

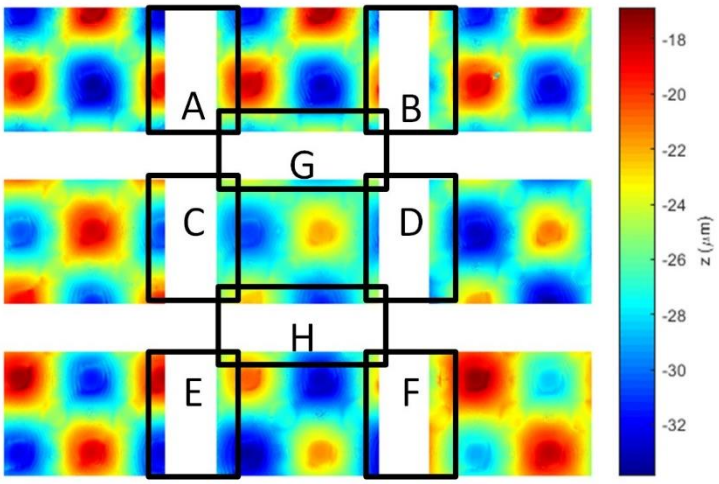

Fig. 10: Mean surfaces of Gaussian process (measurement size of each dataset is approximately (0.3×0.2) mm and the colour bar gives height information in micrometres) and overlapped regions

The mean surfaces were then converted to the grayscale images and the image registration was conducted among the eight overlapped regions (which are highlighted in Fig. 10 with

notions of A to H). Fig. 11 shows the registration results of the overlapped regions for region A. The results show that the sub-surfaces are well registered.

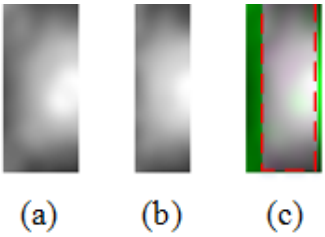

Fig. 11: One pair of the image registration result. (a) fixed image, (b) moving image, (c) registered pair images

After image registration for the *x*-*y* plane, the next step was to perform *z* axis alignment. After that, the coordinate transformation information for all the three axes were obtained and the registration process was finished. In this study, the *z* axis alignment was divided into two steps. The first step was to align the sub-surfaces in the horizontal direction and another step was to align the sub-surfaces in the vertical direction. The horizontal direction step aims to register the sub-surface in the horizontal direction, i.e. region A and B, region C and D, region E and F as shown in Fig. 10. The vertical direction step aims to register the sub-surface in the vertical direction, i.e. region G and H. As a result, the relationship of all the sub-surfaces were determined.

4.2 Result and discussion

After registration, the overlapped data was fused together by using the edge intensity method. Fig. 12 shows the final stitching result after data fusion while Fig. 13 shows the stitching result provided by the CSI software. The detail of the stitching result from the proposed method and that from the CSI software is also shown in Fig. 12(b, c) and Fig. 13(b, c). The stitching result shows that the sub-

surfaces are well stitched together and the stitching result provided by the proposed method has better edge transition features than the stitching result provided by the CSI software. Fig. 12(b, c) shows a better transition area than Fig. 13(b, c) at the region near the edge of the original sub-surfaces. This is due to the characteristics of the edge intensity data fusion method, which combines both the features in the overlapped surfaces to generate a fused dataset. This is particularly useful when the two overlapped sub-surfaces have significantly different measurement results due to measurement noise.

The final stitching result is also compared with that measured with a lower magnification setting (20×0.55) in a single shot measurement. To reduce the effect of the measurement noise, especially the different noise level at different magnifications [24], and evaluate the form error of the stitching method, both the results of the stitched measurements and the single shot measurement are bandwidth-matched through a Gaussian filtering. The cut-off spatial wavelength of the Gaussian filter is 0.01 mm. Moreover, the edge area with half a cut-off length is removed since this area has a large edge effect, which significantly affects the evaluation of the results. The two filtered results are then registered with the ICP method and the error map is calculated and shown in Fig. 14. The single shot measurement has a measurement area of (0.6×0.4) mm which covers the centre part of the final stitching measurement result and contains all the edges in the stitching result. The RMS error with our method is 0.31 μm. Similarly, the stitching result provided by CSI software was also registered to the single shot measurement result using the same method and the error map was obtained and shown in Fig. 15. The RMS error is 0.27 μm. The result shows that the errors are of the same order and both are evenly distributed.

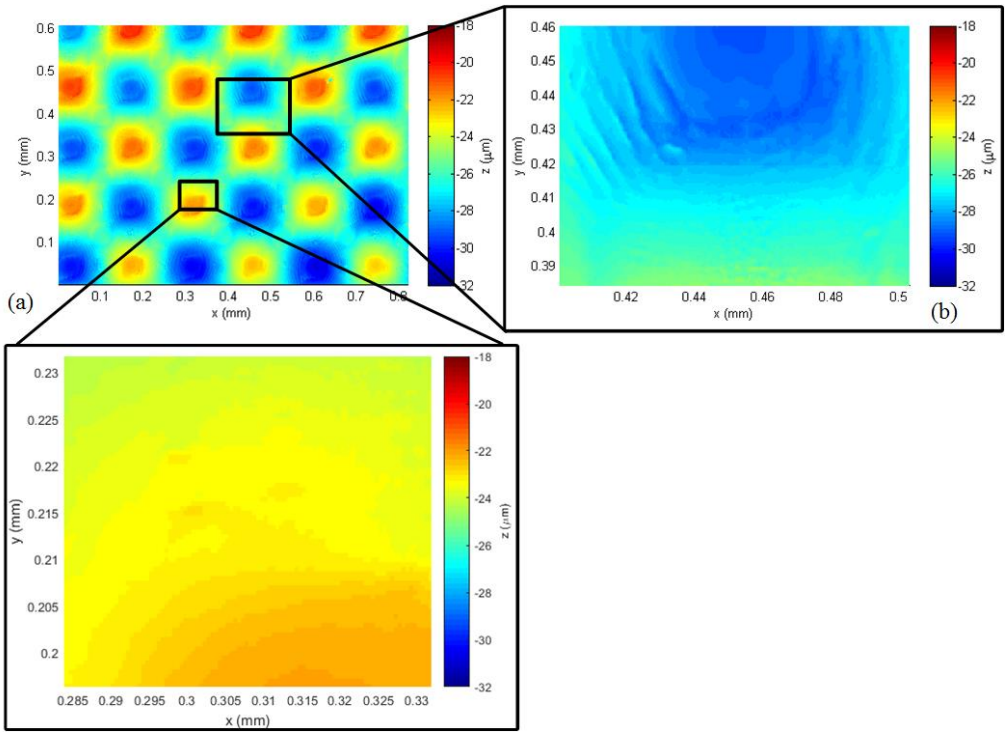

Fig. 12: Stitching result of the proposed method

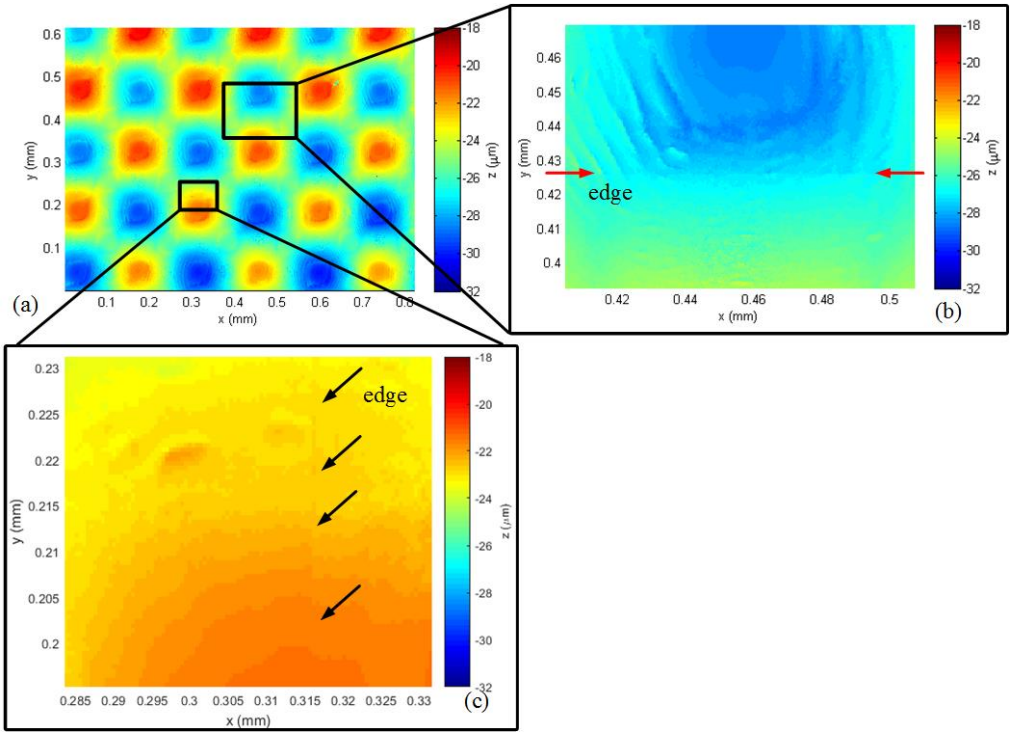

Fig. 13: Stitching result of the CSI software

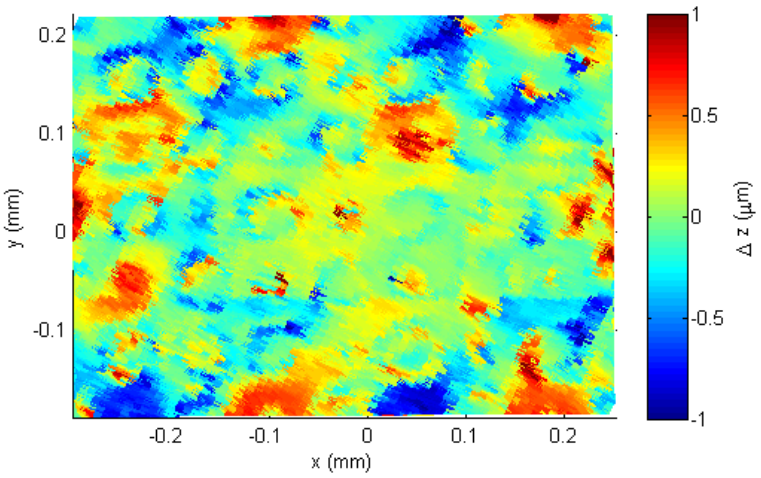

Fig. 14: Proposed stitching error comparing with a single shot measurement

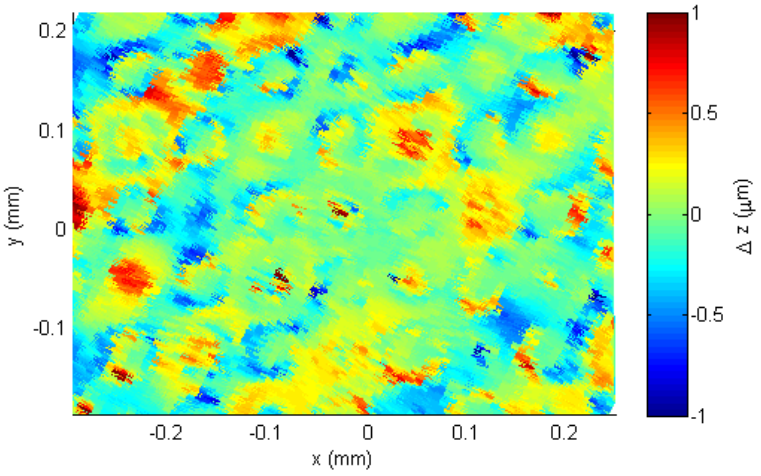

Fig. 15: CSI stitching error comparing with a single shot measurement

The proposed stitching method makes use of a precision moving stage to simplify the stitching process from a 6 DOF problem to 3 DOF problem. For the stitching strategy as shown in the measurement experiment, the length of each sub-surface is about 0.3 mm, to achieve the sub-micrometer stitching accuracy, the angular motion error can be calculated to be less than $\arctan(\frac{0.1\ \mu m}{0.3\ mm}) = 0.33\ mrad$. This requirement can be achieved by many commercial linear stages such as those from Aerotech [25], which rotation error is as small as 50 μrad.

The proposed stitching method is a generic method which is suitable for measuring various kinds of surfaces with different patterns or different local curvature. However, its measurement

ability is affected by the measuring range of the sensor and the moving stage. For the experiments as demonstrated in this study, the measurement ability is limited by the hardware of the instrument: measurement range in the z direction of the CSI and the X-Y stage, which results in the fact that it can only measure surfaces which are relatively flat. With the help of additional rotational stages, the measurement for high-departure aspheres is possible with the modified proposed method. The corresponding translation motion should be modified to the rotation motion. For some kind of surfaces with relatively less features such as those with longer spatial period, the registration accuracy may be largely affected, a pre-processing can be implemented to improve the registration accuracy by using the invariant features such as Gaussian curvature [26]. This will be considered in future work. On the other hand, for some workpiece without strong periodical patterns, the small local difference caused by surface roughness and discontinuity of materials can still be treated as features to ensure the registration accuracy [27].

5. Conclusion

A stitching method for high dynamic range optical measurement of precision surfaces is presented, which is based on a Gaussian process, image registration and data fusion techniques. For the overlapped areas, the data are fused with the edge intensity method. A simulation and actual measurement were conducted for the verification of the method. For both simulation and actual measurements, nine (3×3) sub-surface measurements were stitched together to form a holistic measurement result. The stitching result shows improved edge transition features in the overlapped area, which is an advantage, especially for overlapped sub-surface measurements that have significantly different results. It is concluded that the proposed method is technically feasible and suitable for sub-aperture stitching for large area measurement with optical instruments.

6. Acknowledgments

The authors would like to express their sincere thanks to the Research Committee of The Hong Kong Polytechnic University for the financial support of the project by a PhD studentship (project account code: RTHC). The work described in this paper was also partially supported by a grant from the Research Grants Council (Project No. PolyU 15202814) of the Government of the Hong Kong Special Administrative Region, China. The authors would like to thank Prof. David Robertson from Durham University for providing the diamond turned workpiece and Dr. Wenguang Hou from Huazhong University of Science and Technology for the valuable discussion.

References

[1] Leach RK, Jones CW, Sherlock B, Krysinski A. The high dynamic range surface metrology challenge. 28th Annual Meeting of the American Society for Precision Engineering. St. Paul, Minnesota, USA2013. p. 149-52.
[2] Bray M. Stitching interferometer for large plano optics using a standard interferometer. Optical Science, Engineering and Instrumentation'97: International Society for Optics and Photonics, 1997. p. 39-50.
[3] Liang C-W, Chang H-S, Lin P-C, Lee C-C, Chen Y-C. Vibration modulated subaperture stitching interferometry. Opt Express. 2013;21:18255-60.
[4] Chen S, Li S, Dai Y. Iterative algorithm for subaperture stitching interferometry for general surfaces. JOSA A. 2005;22:1929-36.
[5] Chen S, Xue S, Dai Y, Li S. Subaperture stitching test of large steep convex spheres. Opt Express. 2015;23:29047-58.
[6] Jansen M, Schellekens P, Haitjema H. Development of a double sided stitching interferometer for wafer characterization. CIRP Annals-Manufacturing Technology. 2006;55:555-8.
[7] Preibisch S, Saalfeld S, Tomancak P. Globally optimal stitching of tiled 3D microscopic image acquisitions. Bioinformatics. 2009;25:1463-5.
[8] Chen S, Li S, Dai Y, Zheng Z. Testing of large optical surfaces with subaperture stitching. Applied optics. 2007;46:3504-9.
[9] Zhang L, Liu D, Shi T, Yang Y, Chong S, Ge B, et al. Aspheric subaperture stitching based on system modeling. Opt Express. 2015;23:19176-88.
[10] Ye S-w, Yang P, Peng Y-f. A profile measurement method of large aspheric optical surface based on optimal stitching planning. Precision Engineering. 2016;45:90-7.
[11] Wiegmann A, Stavridis M, Walzel M, Siewert F, Zeschke T, Schulz M, et al. Accuracy evaluation for sub-aperture interferometry measurements of a synchrotron mirror using virtual experiments. Precision engineering. 2011;35:183-90.
[12] Fleig J, Dumas P, Murphy PE, Forbes GW. An automated subaperture stitching interferometer workstation for spherical and aspherical surfaces. Optical Science and Technology, SPIE's 48th Annual Meeting: International Society for Optics and Photonics, 2003. p. 296-307.

[13] Besl PJ, McKay ND. A method for registration of 3-D shapes. IEEE Transactions on pattern analysis and machine intelligence. 1992;14:239-56.
[14] Marinello F, Bariani P, De Chiffre L, Hansen HN. Development and analysis of a software tool for stitching three-dimensional surface topography data sets. Meas Sci Technol. 2007;18:1404-12.
[15] Williams CK, Rasmussen CE. Gaussian processes for machine learning: the MIT Press, 2006.
[16] Gonzalez RC, Woods RE, Eddins SL. Digital image processing using MATLAB: Pearson Education India, 2004.
[17] Wyant JC, Schmit J. Large field of view, high spatial resolution, surface measurements. International Journal of Machine Tools and Manufacture. 1998;38:691-8.
[18] Huang J, Wang Z, Gao J, Huang Y, Towers DP. High-Precision Registration of Point Clouds Based on Sphere Feature Constraints. Sensors. 2016;17:72.
[19] Brinkmann S, Bodschwinna H, Lemke H-W. Accessing roughness in three-dimensions using Gaussian regression filtering. International Journal of Machine Tools and Manufacture. 2001;41:2153-61.
[20] Liu M, Cheung FC, Cheng C-H, Lee BW. A Gaussian Process Data Modelling and Maximum Likelihood Data Fusion Method for Multi-Sensor CMM Measurement of Freeform Surfaces. Applied Sciences. 2016;6.
[21] Rasmussen CE, Nickisch H. Gaussian processes for machine learning (GPML) toolbox. The Journal of Machine Learning Research. 2010;11:3011-5.
[22] Wang J, Leach RK, Jiang X. Review of the mathematical foundations of data fusion techniques in surface metrology. Surface Topography: Metrology and Properties. 2015;3:023001.
[23] Chen H, Liu Y-y, Wang Y-j. A novel image fusion method based on wavelet packet transform. Knowledge Acquisition and Modeling Workshop, 2008 KAM Workshop 2008 IEEE International Symposium on: IEEE, 2008. p. 462-5.
[24] Liu M, Cheung CF, Ren M, Cheng C-H. Estimation of measurement uncertainty caused by surface gradient for a white light interferometer. Applied Optics. 2015;54:8670-7.
[25] Aerotech Inc. Specifications of ANT130-XY Series Two-Axis XY Direct-Drive Nanopositioning Stages. 2017.
[26] Ren MJ, Cheung CF, Kong LB, Jiang XQ. Invariant-Feature-Pattern-Based Form Characterization for the Measurement of Ultraprecision Freeform Surfaces. Ieee T Instrum Meas. 2012;61:963-73.
[27] Liu M, Cheung CF, Chen S. A rotational stitching method for measuring cylindrical surfaces. euspen's 16th International Conference & Exhibition. Nottingham, UK2016.

Figure Caption